

Supporting Information

High Performance 5-Aminotetrazole-based Energetic MOF and Its Catalytic Effect on Decomposition of RDX

Xiaoni Qu, Qi Yang, Jing Han, Qing Wei, Gang Xie, Sanping Chen*, Shengli Gao

*Key Laboratory of Synthetic and Natural Functional Molecule Chemistry of Ministry of Education,
College of Chemistry and Materials Science, Northwest University, Xi'an 710069, China*

Table of Contents:

1.1. X-ray crystallography

Table S1. Crystallographic data for **1**.

Table S2. Selected bond lengths (\AA) and bond angles ($^\circ$) for **1**.

Table S3. Data needed for kinetic calculation of the decomposition process from the TG curves under different heating rates.

Table S4. Apparent activation energies of **1** of the decomposition process obtained using model-free isoconversional methods.

Table S5. Kinetic parameters obtained for the decomposition process of **1**.

Fig. S1. XRPD curve for compound **1**.

Fig. S2. TG curve of **1**.

Fig. S3. $T \sim \alpha$ curves for the decomposition process of **1** at different heating rates.

Fig. S4. $E_a \sim \alpha$ curves for the decomposition process of **1** using different methods.

Fig. S5. The $y(\alpha)$ and $z(\alpha)$ curves based on the obtained kinetic mechanism function.

Fig. S6. DSC curves of **1** under different heating rates.

1.2. Non-isothermal kinetics

1.3. Sensitivity test

1.4. Oxygen bomb calorimetry

1.5. Heat of detonation

References

1.1 X-ray crystallography

Crystallographic data of **1** were collected on a Bruker Smart Apex CCD diffractometer equipped with graphite monochromatized Mo $K\alpha$ radiation ($\lambda = 0.71073 \text{ \AA}$) using ω and φ scan mode. The single-crystal structure of **1** was solved using direct methods by SHELXS-97,^[1] and refined by means of full-matrix least-squares procedures on F^2 with SHELXL-97^[2] crystallographic program. All non-H atoms were located using subsequent Fourier-difference methods and refined anisotropically. In all cases, hydrogen atoms were placed in calculated positions and thereafter allowed to ride on their parent atoms. The crystal data and structure refinement details of compound are summarized in Table S1, while the selected bond lengths and angles data are presented in Table S2. XRPD indicated that **1** was crystalline state, confirming the phase purity of the compound (Fig. S1). The crystal structure has been deposited in the Cambridge Crystallographic Data Centre, with CCDC 1433471. These data can be obtained free of charge from The Cambridge Crystallographic Data Centre via www.ccdc.cam.ac.uk/data_request/cif.

Table S1. Crystallographic data for **1**.

Compound	1
CCDC	1433471
Empirical formula	$\text{Ag}_2\text{CH}_2\text{N}_8$
Formula weight	341.85
Crystal system	Orthorhombic
space group	<i>Pbam</i>
<i>a</i> (\AA)	16.3005(7)
<i>b</i> (\AA)	6.3588(2)
<i>c</i> (\AA)	6.4725(3)
α ($^\circ$)	90
β ($^\circ$)	90
γ ($^\circ$)	90
<i>V</i> (\AA^3)	670.89(5)
<i>Z</i>	4

D_c (g cm ⁻³)	3.384
T (K)	153(2)
μ (mm ⁻¹)	5.777
$F(000)$	632
Reflections collected/unique	3518 / 652
$R(\text{int})$	0.0198
Data/restraints/parameters	652 / 3 / 66
GOF ^c on F^2	1.833
R_1 ^a [$I > 2\sigma(I)$]	0.0426
wR_2 ^b (all data)	0.2145

^a $R_1 = \sum ||F_o| - |F_c|| / \sum |F_o|$; ^b $wR_2 = [\sum w(F_o^2 - F_c^2)^2 / \sum w(F_o^2)]^{1/2}$.

^c GOF = goodness of fit.

Table S2. Selected bond lengths (Å) and bond angles (°) for **1**.

Ag(1)-N(1)#1	2.256(4)	N(4)#2-Ag(1)-Ag(1)#2	51.35(10)
Ag(1)-N(1)	2.256(4)	N(4)-Ag(1)-Ag(1)#2	51.35(10)
Ag(1)-N(4)#2	2.383(5)	N(2)#3-Ag(2)-N(2)#4	150.3(3)
Ag(1)-N(4)	2.383(5)	N(2)#3-Ag(2)-N(4)	101.04(13)
Ag(1)-Ag(1)#2	2.976(3)	N(2)#4-Ag(2)-N(4)	101.04(13)
Ag(2)-N(2)#3	2.229(5)	N(2)#3-Ag(2)-N(6)#5	101.00(14)
Ag(2)-N(2)#4	2.229(5)	N(2)#4-Ag(2)-N(6)#5	101.00(14)
Ag(2)-N(4)	2.496(7)	N(4)-Ag(2)-N(6)#5	83.5(2)
Ag(2)-N(6)#5	2.501(8)	N(1)#6-N(1)-Ag(1)	118.80(10)
N(2)-Ag(2)#3	2.229(5)	N(2)-N(1)-Ag(1)	132.6(4)
N(4)-Ag(1)#2	2.383(5)	N(1)-N(2)-Ag(2)#3	123.3(4)
N(6)-Ag(2)#7	2.501(8)	C(1)-N(2)-Ag(2)#3	129.5(5)
N(1)#1-Ag(1)-N(1)	122.4(2)	N(5)-N(4)-Ag(1)#2	116.0(4)
N(1)#1-Ag(1)-N(4)#2	114.58(19)	N(5)-N(4)-Ag(1)	116.0(4)
N(1)-Ag(1)-N(4)#2	100.71(18)	Ag(1)#2-N(4)-Ag(1)	77.3(2)

N(1)#1-Ag(1)-N(4)	100.71(18)	N(5)-N(4)-Ag(2)	116.8(5)
N(1)-Ag(1)-N(4)	114.58(19)	Ag(1)#2-N(4)-Ag(2)	112.3(2)
N(4)#2-Ag(1)-N(4)	102.7(2)	Ag(1)-N(4)-Ag(2)	112.3(2)
N(1)#1-Ag(1)-Ag(1)#2	118.80(10)	N(5)-N(6)-Ag(2)#7	131.8(6)
N(1)-Ag(1)-Ag(1)#2	118.80(10)		

Symmetry transformations used to generate equivalent atoms:

#1 -x+1,-y-1,z; #2 -x+1,-y-1,-z; #3 -x+1,-y,-z; #4 -x+1,-y,z;

#5 -x+1/2,y+1/2,z; #6 x,y,-z-1; #7 -x+1/2,y-1/2,z.

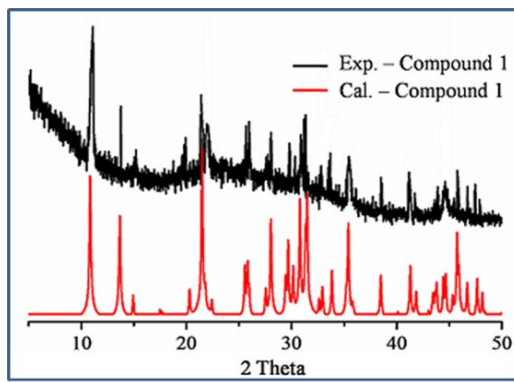


Fig. S1. XRPD curve for compound 1.

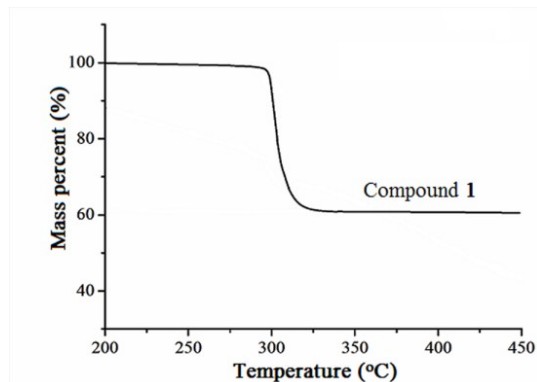


Fig. S2. TG curve of 1.

1.2 Non-isothermal kinetics

In our present work, iso-conversional kinetic method^[3] was employed to estimate the kinetic triplets (the apparent activation energy (E_a), the preexponential factor (A) and the mechanism function ($f(\alpha)$)) according to the degree of conversion/reaction (α). The TG-DTG data with the

heating rates of 2, 5, 8 and 10 °C min⁻¹ were collected in Table S3 and the $T\sim\alpha$ curves with different heating rates and $E_a\sim\alpha$ curves by using different methods were plotted in Fig. S3-S4. The methods for obtaining E_a are deduced from the following four equations (1)-(4),^[3b-3f]

Integral isoconversional non-linear [NL-INT₀] equation,^[3b]

$$\left| \sum_i^n \sum_{j \neq i}^n \frac{\beta_j(T_i - T_{0,i}) \exp(-E_a/RT_i)}{\beta_i(T_j - T_{0,j}) \exp(-E_a/RT_j)} - n(1-n) \right| = \min \quad (1)$$

Integral isoconversional non-linear [NL-INT] equation,^[3c]

$$\left| \sum_i^n \sum_{j \neq i}^n \frac{\beta_j I(E_a T_{a,i})}{\beta_i I(E_a T_{a,j})} - n(n-1) \right| = \min \quad (2)$$

Flynn-Wall-Ozawa (F-W-O) equation,^[3d,3e]

$$\lg \beta = \lg \left(\frac{AE}{RG(\alpha)} \right) - 2.315 - 0.4576 \frac{E}{RT} \quad (3)$$

Kissinger equation,^[3f]

$$\ln \frac{\beta}{T_p^2} = \ln \frac{AR}{E} - \frac{E}{RT_p} \quad (4)$$

Where α is the degree of conversion/reaction, T is the absolute temperature (K), T_0 is the beginning temperature deviating the baseline (K), E_a is the apparent activation energy (kJ mol⁻¹), β is the heating rates (°C min⁻¹), A is the preexponential factor (s⁻¹), $G(\alpha)$ is the mechanism function and $R = 8.314$ J mol⁻¹ K⁻¹.

Additionally, based on the five kinetic analysis methods (Ordinary integral, Uivenrsal integral, Mac Collum-Tanner, Šatava-Šesták and Agrawal) reported in Ref 3, the average E_a and $\log A$ are respectively 291.8 kJ mol⁻¹ and 24.0402 s⁻¹. The probable kinetic mechanism function ($f(\alpha)$) was selected *via* the optimal value of r , and Q , and the $f(\alpha)$ and the kinetic equation are described as equations (5) and (6),

$$f(\alpha) = 2(1 - \alpha)[- \ln(1 - \alpha)]^{1/2} \quad (5)$$

$$\frac{d\alpha}{dT} = \frac{2.1940 \times 10^{24}}{\beta} (1 - \alpha)[- \ln(1 - \alpha)]^{1/2} \exp\left(-\frac{3.5094 \times 10^4}{T}\right) \quad (6)$$

Additionally, according to the Ref. 4 and the above kinetic mechanism function ($f(\alpha)$), the $y(\alpha)$ and $z(\alpha)$ functions can be expressed as equations (7)-(9). The $y(\alpha)$ and $z(\alpha)$ curves are shown in the Fig. S5, which further proves that the position and shape should be approximately invariant when changing heating rate (nonisothermal conditions) and temperature (isothermal conditions).

$$g(\alpha) = [- \ln(1 - \alpha)]^{1/2} \quad (7)$$

$$y(\alpha) = B_n f(\alpha) = 2B_n(1 - \alpha)[- \ln(1 - \alpha)]^{1/2} \quad (8)$$

$$z(\alpha) = C_n f(\alpha) g(\alpha) = 2C_n(1 - \alpha)[- \ln(1 - \alpha)] \quad (9)$$

Where B_n and C_n are constants, and α is the degree of conversion/reaction.

DSC experiments with the heating rates of 2, 5, 8 and 10 °C min⁻¹ were carried out and the values (T_{00} , T_{e0} and T_{p0}) of the initial temperature point corresponding to $\beta \rightarrow 0$ are obtained by equation (10)^[5] from the DSC curves (Fig. S6). The equations (11) and (12) are applied to obtain the values of the self-accelerating decomposition temperature (T_{SADT}) and critical temperature of thermal explosion (T_b) for **1**. The T_{SADT} and T_b are respectively 280.3 °C and 289.2 °C, revealing more perfect thermal stability in the exothermic decomposition stage than common explosives and the known energetic compounds.

$$T_{(0, e \text{ or } p)i} = T_{(00, e0 \text{ or } p0)i} + n\beta_i + m\beta_i^2 \quad i = 1 - 4 \quad (10)$$

$$T_{SADT} = T_{e0} \quad (11)$$

$$T_b = \frac{E_0 - \sqrt{E_0^2 - 4E_0RT_{e0}}}{2R} \quad (12)$$

Table S3. Data needed for kinetic calculation of the decomposition process from the TG curves under different heating rates.

α	T_i (K)			
	2 (°C min ⁻¹)	5 (°C min ⁻¹)	8 (°C min ⁻¹)	10 (°C min ⁻¹)
	$T_0=552.76$	$T_0=558.13$	$T_0=563.13$	$T_0=565.27$
0.00573	555.70	561.52	566.06	568.84
0.00739	556.53	561.86	566.47	569.73
0.00941	557.81	563.13	568.26	570.52
0.02081	558.08	564.41	568.54	571.84
0.04015	558.36	564.69	569.82	573.08
0.06722	559.27	565.60	570.72	573.98
0.10204	560.36	566.69	572.32	575.07
0.14461	562.09	568.42	573.23	575.81
0.19363	562.63	568.97	574.09	576.35
0.24606	563.37	569.91	574.83	578.08
0.29825	565.08	570.81	575.54	578.80
0.34862	565.63	572.45	577.09	579.83
0.39911	566.36	573.18	577.82	580.57
0.45383	568.10	573.92	578.55	581.3
0.51554	568.83	574.65	580.29	583.03
0.58247	569.19	576.01	581.13	583.67
0.64856	570.73	577.55	581.68	584.43

0.70683	571.28	578.44	583.22	585.97
0.75351	572.82	579.13	583.77	586.52
0.78978	573.37	579.68	585.32	587.40
0.81992	574.92	581.22	586.14	589.10
0.84778	575.65	581.96	587.08	589.83
0.87454	576.19	582.82	587.63	590.77
0.89917	577.93	583.72	588.51	591.60
0.92057	578.47	585.27	589.40	593.14
0.9391	580.02	585.81	590.94	593.18
0.95588	580.75	587.55	591.68	594.91
0.9712	581.30	588.09	592.43	595.95
0.98371	582.84	589.02	594.26	596.68
0.99156	583.75	590.54	595.16	597.77
0.99443	584.29	591.58	596.19	598.92

(α) the degree of conversion/reaction, (T_i) the temperature at the different heating rates and (T_0) the beginning temperature from the TG curves.

Table S4. Apparent activation energies of the title compound of the decomposition process obtained using model-free isoconversional methods.

No	α	E_a (kJ mol ⁻¹)			
		Kissinger's method	Flynn-Wall-Ozawa's method	NL-INT's method	NL-INT ₀ 's method
1	0.00573	313.99	307.47	314.11	310.94
2	0.00739	312.77	306.33	312.89	314.86
3	0.00941	319.66	312.90	319.79	329.44
4	0.02081	306.83	300.70	306.95	295.14
5	0.04015	282.55	277.63	282.69	245.28
6	0.06722	283.72	278.76	283.86	252.45
7	0.10204	280.92	276.11	281.06	251.11
8	0.14461	306.56	300.51	306.69	298.45
9	0.19363	304.10	298.19	304.24	294.75
10	0.24606	289.24	284.07	289.38	270.80
11	0.29825	310.96	304.74	311.08	308.77
12	0.34862	302.04	296.27	302.17	292.95
13	0.39911	302.65	296.86	302.78	294.39
14	0.45383	326.07	319.16	326.20	331.55
15	0.51554	298.28	292.76	298.42	291.0
16	0.58247	297.01	291.55	297.16	287.98
17	0.64856	321.01	314.39	321.14	322.10
18	0.70683	297.61	292.16	297.75	289.46
19	0.75351	320.42	313.87	320.56	322.06
20	0.78978	305.16	299.37	305.31	301.53
21	0.81992	311.16	305.10	311.30	309.73
22	0.84778	310.21	304.20	310.35	308.56

23	0.87454	305.67	299.90	305.81	302.33
24	0.89917	325.93	319.18	326.06	329.62
25	0.92057	310.76	314.77	310.89	308.99
26	0.9391	335.43	328.25	335.56	341.60
27	0.95588	323.34	316.77	323.47	325.05
28	0.9712	312.95	306.90	313.09	312.04
29	0.98371	323.40	316.86	323.54	325.75
30	0.99156	325.36	318.74	325.5	327.57
31	0.99443	313.32	307.30	313.46	312.35
Mean (4-23)		303.11	297.32	303.25	293.52

(α) the degree of conversion/reaction and (E_a) apparent activation energy.

Table S5. Kinetic parameters obtained for the decomposition process of the title compound.

Methods	β (°C min ⁻¹)	E_a (kJ mol ⁻¹)	log A (s ⁻¹)	R	Q	d	Function
							No.
Ordinary integral	2	284.18	25.5544	0.9641675	0.5632544	0.02018279	13
	5	287.47	23.9547	0.9645175	0.5578383	0.01979352	13
	8	292.39	24.3803	0.9671766	0.5168263	0.01696401	13
	10	299.70	25.0120	0.9613357	0.6081137	0.02351229	13
Uivenrsal integral	2	290.43	22.1643	0.9656317	0.5629607	0.01934803	13
	5	293.78	22.5649	0.9659649	0.5575510	0.01897633	13
	8	298.74	22.9874	0.9685105	0.5165200	0.01626495	13
	10	306.08	23.6112	0.9628605	0.6078023	0.02257346	13
Mac Collum-Tanner	2	287.05	23.8906	0.9663489	0.1061362	0.00357159	13
	5	290.47	24.3062	0.9666777	0.1051167	0.00350272	13
	8	295.50	24.7476	0.9691710	0.0973747	0.00300196	13
	10	302.92	25.3961	0.9636178	0.1145908	0.00416906	13
Šatava-Šesták	2	279.21	23.1706	0.96634891	0.1061362	0.00357159	13
	5	282.43	23.5707	0.9666777	0.1051167	0.00350272	13
	8	287.19	23.9892	0.9691710	0.0973747	0.00300196	13
	10	294.19	24.6045	0.9636178	0.1145908	0.00416906	13
Agrawal	2	284.18	23.5538	0.9641675	0.5632544	0.02018279	13
	5	287.47	23.9541	0.9645175	0.5578383	0.01979352	13
	8	292.39	24.3797	0.9671766	0.5168263	0.01696401	13
	10	299.70	25.0114	0.9613357	0.6081137	0.02351229	13
Mean		291.77	24.0402	0.96545			

(β) the heating rates, (E_a) apparent activation energy, (A) pre-exponential factor, (R) linear correlation coefficient, (Q) standard mean square deviation and (d) believable factor ($d=(1-\alpha)Q$).

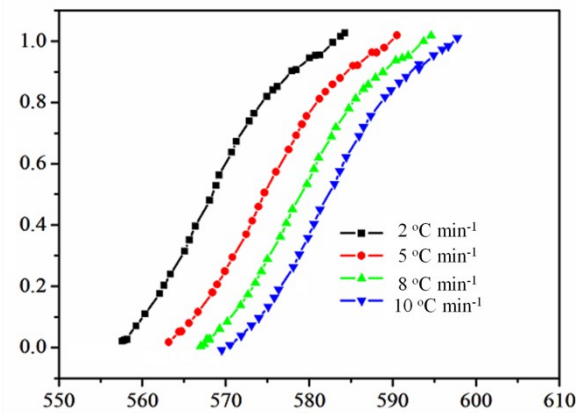


Fig. S3. $T \sim \alpha$ curves for the decomposition process of **1** at different heating rates.

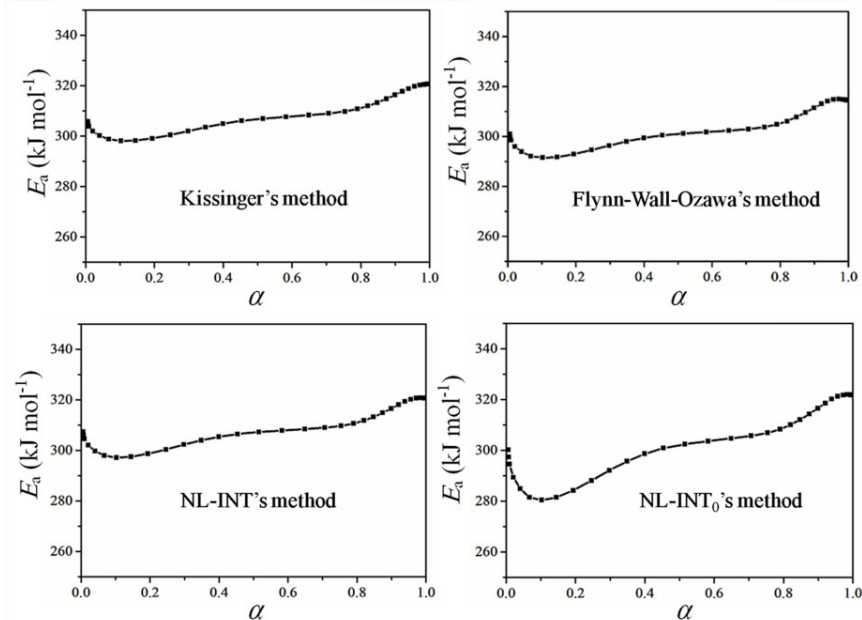


Fig. S4. $E_a \sim \alpha$ curves for the decomposition process of **1** using different methods.

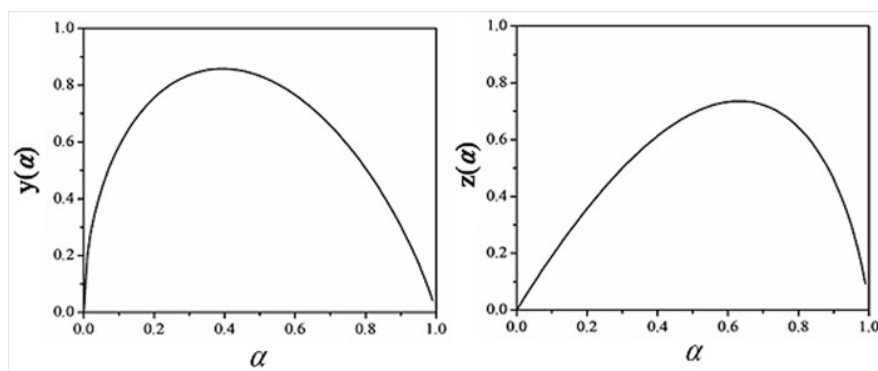


Fig. S5. The $y(\alpha)$ and $z(\alpha)$ curves based on the obtained kinetic mechanism function.

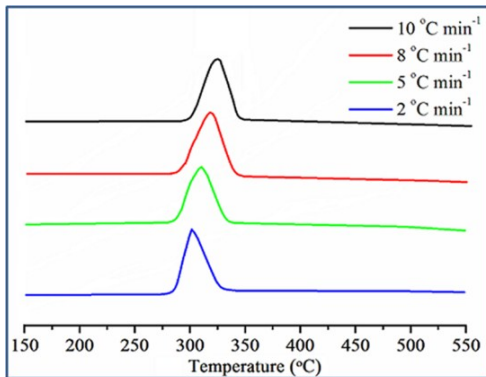


Fig. S6. DSC curves of **1** under different heating rates.

1.3 Sensitivity test

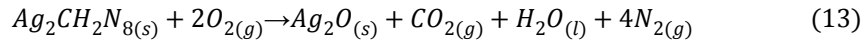
Impact sensitivity was determined by Fall Hammer Apparatus. Twenty milligrams of the compound was compacted to a copper cap under the press of 39.2 MPa, and was hit by 2 kg drop hammer, and the calculated value of h_{50} represents the drop height of 50% initiation probability. The impact sensitivity value of **1** is measured to be 200 cm, which corresponds to the impact energies of 40 J.

Friction sensitivity of the compound was measured by applying a Julius Peter's machine using 20 mg sample. No friction sensitivity is observed up to 36 kg (360 N) for **1**.

1.4 Oxygen bomb calorimetry

The constant-volume combustion energies of **1** was investigated by a precise rotating-oxygen bomb calorimeter (RBC-type II).^[6] Approximately 10 mg of the samples were pressed with a well-defined amount of benzoic acid (Calcd. 30 mg) to form a tablet to ensure better combustion. The recorded data are the average of six single measurements. The calorimeter was calibrated by the combustion of certified benzoic acid (Standard Reference Material, 39i, NIST) in an oxygen atmosphere at a pressure of 30.5 bar. The experimental value of the constant volume combustion energies ($\Delta_c U$) for **1** was $(-4522.45 \pm 2.47) \text{ J g}^{-1}$. Then the enthalpies of combustion ($\Delta_c H^\theta_m$) was calculated as $(-1539.46 \pm 0.84) \text{ kJ mol}^{-1}$ on the basis of the formula $\Delta_c H^\theta_m = \Delta_c U^\theta_m + \Delta n RT$, $\Delta n = n_g(\text{products}) - n_g(\text{reactants})$, (n_g is the total molar amount of gases in the products or reactants, $R = 8.314 \text{ J mol}^{-1} \text{ K}^{-1}$, $T = 298.15 \text{ K}$). Subsequently, according to combustion reaction equation (13), Hess's law in thermochemical equation (14) and the known enthalpies of formation of the combustion products^[7] $\text{Ag}_2\text{O(s)}$, $\Delta_c H^\theta_m (\text{Ag}_2\text{O, s}) = -31 \text{ kJ mol}^{-1}$, $\text{CO}_2(\text{g})$, $\Delta_c H^\theta_m (\text{CO}_2, \text{g}) = (-$

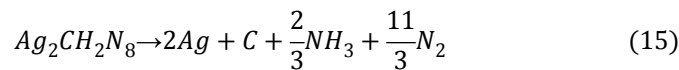
393.51 ± 0.13 kJ mol⁻¹, H₂O (l), $\Delta_c H_m^0$ (H₂O, l) = (-285.830 ± 0.040) kJ mol⁻¹, the standard enthalpies of formation for **1** ($\Delta_f H_m^0$) is obtained as (829.12 ± 0.84) kJ mol⁻¹, evidencing that N-N, N=N bonds and azido group in structure make a decisive contribution to the enthalpy of formation of **1**.



$$\Delta_f H_{m(s)}^0 = \Delta_f H_{m(Ag_2O, s)}^0 + \Delta_f H_{m(CO_2, g)}^0 + \Delta_f H_{m(H_2O, l)}^0 - \Delta_c H_{m(1, s)}^0 \quad (14)$$

1.5 Detonation properties

In the current work, on the basis of the largest exothermic principle proposed by Kamlet-Jacobs,^[8] we employed an empirical method previously reported^[7a,9] to investigate the energetic performances of metal-containing explosives without depending on sophisticated computer programs. The new and efficient method, which employed the hypothesis of BKW equation and arbitrary theory of the K-J method, could be applied to perform the detonation performances of metal compounds containing special elements such as Cd and Ag. The Kamlet-Jacobs equations and detonation reaction of **1** are as shown in equation (15-19). The heat of detonation value ($Q/J\text{ g}^{-1}$), detonation pressure (P) and detonation velocity (D) of **1** are respectively calculated as 0.6 kcal g⁻¹, 7.0 km s⁻¹ and 29.5 GPa.



$$D = 1.01\Phi^{1/2}(1 + 1.30\rho) \quad (16)$$

$$P = 1.558\Phi\rho^2 \quad (17)$$

$$\Phi = 31.68N(MQ)^{1/2} \quad (18)$$

$$Q = \frac{-[\Delta H_f(\text{detonation products}) - \Delta H_f(\text{explosive})]}{\text{formula weight of explosive}} \quad (19)$$

Where D represents detonation velocity (km s⁻¹), P is detonation pressure (GPa), ρ is the density of explosive (g cm⁻³), N is the moles of detonation gases per gram of explosive (mol g⁻¹), M is the average molecular weight of these gases (g mol⁻¹), Q is the heat of detonation (kcal g⁻¹) and Φ is a characteristic parameter of an explosive.

References

- 1 (a) G. M. Sheldrich, *Acta Crystallogr., Sect. A: Found. Crystallogr.* 1990, **46**, 467. (b) G. M. Sheldrick, *Acta Cryst.*, 2008, **A64**, 112-122.
- 2 (a) W. Madison, Bruker APEX2 Software, V2.0-1; Bruker AXS Inc.: Fitchburg, WI, 2005. (b) G. M. Sheldrick, SHELXL-97, Program for X-ray Crystal Structure Refinement, University of Göttingen, Germany, 1997.
- 3 (a) S. Vyazovkin, A. K. Burnham, J. M. Criado, L. A. Pérez-Maqueda, C. Popescu and N. Sbirrazzuoli, *Thermochim. Acta*, 2011, **520**, 1-19. (b) R. Z. Hu and Q.Z. Shi, Science Press, Beijing, 2001. (c) S. Vyazovkin and D. Dollimore, *J. Chem. Information Comp. Sci.*, 1996, **36**, 42-45. (d) J. H. Flynn and L. A. Wall, *J. Polym. Sci.*, Part B, *Polym. Lett.*, 1966, **4**, 323-328. (e) T. Ozawa, *Bull. Chem. Soc. Jpn.*, 1965, **38**, 1881-1886. (f) H. E. Kissinger, *Anal. Chem.*, 1957, **29**, 1702-1706. (g) B. J. Jiao, S. P. Chen, F. Q. Zhao, R. Z. Hu and S. L. Gao, *J. Hazard. Mater.*, 2007, **142**, 550-554.
- 4 (a) J. Málek, *Thermochim. Acta*, 2000, **355**, 239-253. (b) J. Málek, *Thermochim. Acta*, 1992, **200**, 257-269. (c) R. Svoboda, J. Málek, *Thermochim. Acta*, 2011, **526**, 237-251. (d) A. Khawam, D. R. Flanagan, *J. Phys. Chem. B*, 2006, **110**, 17315-17328.
- 5 (a) Y. Zhang, H. Wu, K. Z. Xu, W. T. Zhang, Z. Y. Ren, J. R. Song and F. Q. Zhao, *J. Phys. Chem. A.*, 2014, **118**, 1168-1174. (b) H. X. Ma, J. R. Song, F. Q. Zhao, R. Z. Hu and H. M. Xiao, *J. Phys. Chem. A.*, 2007, **111**, 8642-8649.
- 6 X. W. Yang, S. P. Chen, S. L. Gao, H. Li and Q. Z. Shi, *Instrum. Sci. Technol.*, 2002, **30**, 311-321.
- 7 (a) Y. Wang, J. C. Zhang, H. Su, S. H. Li, S. W. Zhang and S. P. Pang, *J. Phys. Chem. A.*, 2014, **118**, 4575-4581. (b) A. Bondi, *J. Phys. Chem.*, 1964, **68**, 441-451.
- 8 (a) M. J. Kamlet and S. Jacobs, *J. Chem. Phys.*, 1968, **48**, 23-35. (b) M. J. Kamlet, J. Ablard, *J. Chem. Phys.*, 1968, **48**, 36-42. (c) M. J. Kamlet, C. Dickinson, *J. Chem. Phys.*, 1968, **48**, 43-50. (d) M. J. Kamlet, H. Hurwitz, *J. Chem. Phys.*, 1968, **48**, 3685-3692.
- 9 S. H. Li, Y. Wang, C. Qi, X. X. Zhao, J. C. Zhang, S. W. Zhang and S. P. Pang, *Angew. Chem. Int. Ed.*, 2013, **52**, 14031-14035.